Article type: Full Paper

Thin film deposition on open-cell foams by atmospheric pressure dielectric barrier discharges

Fiorenza Fanelli,* Francesco Fracassi

Dr. F. Fanelli, Prof. F. Fracassi
National Research Council, Institute of Nanotechnology (CNR-NANOTEC)
c/o Department of Chemistry, University of Bari 'Aldo Moro', via Orabona 4, 70126 Bari, Italy
E-mail: fiorenza.fanelli@cnr.it
Prof. F. Fracassi
Department of Chemistry, University of Bari 'Aldo Moro', via Orabona 4, 70126 Bari, Italy

Thin films are deposited on open-cell polyurethane (PU) foams using an atmospheric pressure dielectric barrier discharge (DBD) fed with helium and hexafluoropropene (C_3F_6). During deposition processes, a foam substrate is sandwiched between the dielectric-covered electrodes of a parallel plate DBD reactor, so that the discharge can ignite also inside its three-dimensional (3D) interconnected porous structure. This affords the deposition of a fluorocarbon coating on both the exterior and interior of the foam. Scanning electron microscopy (SEM) observations allow estimating the thickness of the coating deposited on the foam struts, while X-ray photoelectron spectroscopy (XPS) analyses show moderate changes in surface chemical composition moving from the outer to the inner surfaces of the plasma-treated foams under all explored experimental conditions.

Introduction

In recent years thin film deposition on complex three-dimensional (3D) porous substrates has attracted growing interest in materials chemistry for the design and fabrication of biomaterials,[1] heterogeneous catalysts,[2] special wettable materials,[3] selective adsorbents,[4] etc..

Efforts have been directed towards the preparation of conformal coatings onto the entire 3D network of the substrates, i.e., onto their outer and inner surfaces, while leaving the bulk properties and porous architecture intact. Several strategies have been developed for thin film deposition on a large variety of complex porous materials, such as polymer, metal and ceramic foams or scaffolds. They exploit, for instance, liquid phase reactions as well as dip-, spin- and spray-coating methods.[2-7] Moreover, among various gas phase techniques,[1,8-12] over the last decade, the low pressure plasma-enhanced chemical vapor deposition (PECVD) has demonstrated to be a viable approach for surface modification of porous materials, as for instance widely reported in the case of polymer scaffolds for tissue engineering applications.[1,11-12] Deposition inside porous scaffolds is driven by the non-line-of-sight ability of low pressure plasmas for surface modification of objects with complex 3D geometries. Specifically, diffusion of reactive depositing species into the scaffold interior is thought to control thin film deposition in low pressure PECVD processes.[1,13] Several studies reported, in fact, that limited penetration of thin film precursors within porous 3D structures can result in gradients of both coating thickness and surface chemical composition moving from the exterior to the interior of the plasma-treated substrate.[1,11-12] Treatment uniformity throughout the entire porous structure could be improved if the discharge could ignite inside the substrate pores and, therefore, as for instance with atmospheric pressure operation. In fact, to achieve plasma ignition, pores dimension must be consistently greater than the Debye length, and for substrates having sub-millimeter pore sizes this is unlikely to occurs under low

pressure plasma conditions. In case of a low pressure glow discharge, characterized for instance by electron temperature and electron density of 4 eV and 10^{10} cm^{-3}, respectively, the Debye length is estimated to be 0.14 mm.[14]

The possibility of igniting the atmospheric cold plasma within complex porous structures on millimeter and sub-millimeter scales was already demonstrated for ceramic foams and scaffolds,[15] however, to our best knowledge, the atmospheric pressure PECVD of thin films on complex porous substrates has not been reported so far. Indeed, this possibility could open new and exciting opportunities in plasma processing. In fact, it is worth mentioning that notable examples reported the atmospheric pressure PECVD of thin films onto the inner surfaces of tubes and channels having inner diameter or width ranging between a few hundred microns and a few millimetre;[16] interestingly, the common thread among these studies is that deposition is accomplished by igniting the atmospheric plasma directly inside the tubes or channels to be treated.

This contribution focuses on the atmospheric pressure PECVD of fluorocarbon coatings on commercial open-cell polyurethane (PU) foams using a dielectric barrier discharge (DBD) fed with helium and hexafluoropropene (C_3F_6). The choice of a fluorocarbon coating was motivated by the need to clearly distinguish the deposited layer from the underlying polyurethane substrate when the surface chemical composition of both the exterior and interior of the plasma-treated foams was investigated. In particular in this work, deposition processes were carried out using a parallel plate DBD reactor, while foam substrates were located in the middle of the discharge region, so that the atmospheric plasma could ignite also inside their porous structure. Results from X-ray photoelectron spectroscopy (XPS) and scanning electron microscopy (SEM) analyses confirmed the deposition of a fluorocarbon coating on both the exterior and interior of the plasma-treated foams.

Experimental Section

Deposition processes were carried out using a home-built atmospheric pressure DBD reactor described previously in full detail.[17] The plasma was generated between two parallel plate electrodes (5 mm gas gap, 120 × 120 mm^2 electrode area) both covered with a 0.635 mm thick Al_2O_3 plate (CoorsTek, 96%) by applying a sinusoidal ac high voltage (20 kHz, 1.15 kV_{rms}).[17] A schematic representation of the DBD electrode system is reported in **Figure 1**a. The voltage applied to the electrodes was measured by means of a high-voltage (HV) probe (Tektronix P6015A), while the current flowing through the electrical circuit was evaluated by measuring the drop across a 50 Ω resistor connected in series with the ground electrode (Tektronix P2200 voltage probe). [17] The average power dissipated by the discharge was calculated as the integral over one cycle of the product of the applied voltage and the current, divided by the period.

The DBD electrode system was located into a Plexiglas chamber slightly pumped with a rotary pump (Pfeiffer), to keep the working pressure constant (10^5 Pa) as measured by a MKS capacitive pressure gauge. During the deposition process the atmospheric plasma was fed with He (Airliquide, 99.999%) and hexafluoropropene (Zentek, 99%) at flow rates of 6 slm and 6 sccm, respectively ($[C_3F_6]$ = 0.1%), controlled with MKS mass flow controllers. Before each experiment, the Plexiglas chamber was purged with 6 slm of He for 20 min to remove air contaminations.

The feed mixture was introduced in the discharge zone through a slit and pumped through a second slit positioned on the opposite side (i.e., lateral gas injection), while rectangular quartz bars, oriented parallel to the gas flow direction and placed along the electrode edges, favored gas canalization. Therefore, in the DBD system the feed mixture was allowed to flow through

a channel having rectangular cross-section of 120 mm × 5 mm (i.e., 5 mm gap gap and 120 mm electrode side).

Thin films were deposited on a commercial open-cell polyurethane foam (Modulor GmbH) characterized by polyester polyol-based polyurethane structure, porosity of about 97% and pore density (also referred to as pore count) of 30 pores per inch (ppi). Rectangular foam strips, having length of 120 mm, width of 10 or 30 mm, and thickness of 5 mm, were used as substrates. They were placed in the middle of the discharge region, oriented perpendicularly to the gas flow direction, sandwiched between the dielectric-covered electrodes of the DBD cell (i.e., both foam and gas gap have equal thickness of 5 mm). It is worth highlighting that in this configuration the foam strips had a cross-section perpendicularly to the gas flow direction of 120 cm × 5 mm, while the width of the foam substrate along the gas flow direction was of either 10 mm or 30 mm (Figure 1a).

For comparative experiments thin films were also deposited on 0.15 mm thick borosilicate glass slides located in the middle of the DBD region on the lower dielectric-covered electrode. In this work the duration of the deposition processes (i.e., deposition time) was varied between 5 and 30 min.

X-ray Photoelectron Spectroscopy (XPS) analyses were performed using a Thermo Electron Theta Probe spectrometer equipped with a monochromatic Al Ka X-ray source (1486.6 eV) operated at a spot size of 300 μm corresponding to a power of 70 W. Survey (0–1200 eV) and high resolution (C1s, O1s, N1s and F1s) spectra were recorded in FAT (fixed analyzer transmission) mode at pass energy of 200 and 50 eV, respectively. All spectra were acquired at a take-off angle of 53° with respect to the sample normal. A flood gun was used to balance the surface charging. Charge correction of the spectra was performed by taking the hydrocarbon (C-C/C-H) component of the C1s spectrum as internal reference (binding energy, BE = 284.8 eV). Atomic percentages were calculated from the high resolution spectra using the Scofield sensitivity factors set in the Thermo Avantage software (Thermo Fisher

Corporation, version 5.938) and a non-linear Shirley background subtraction algorithm. The best-fitting of the high resolution C1s spectra was performed using the Thermo Avantage software. To analyze the interior of the samples (i.e. foam cross-section), after plasma treatment the foam strips were cut with a scalpel blade parallel to the gas flow direction and perpendicular to the strip top. The analyses were repeated on three samples produced in different experiments on at least 3-6 positions per sample.

The morphology of the pristine and plasma-treated PU foams was investigated using a Zeiss SUPRA™ 40 field emission scanning electron microscope (FESEM). SEM images were acquired with a Everhart-Thornley detector at the working distance in the range 8.5-9.5 mm, electron acceleration voltage (extra-high tension, EHT) of 3 kV, magnification in the range 0.1-40 k×. Substrates were sputter-coated with a 20 nm thick layer of Cr prior to SEM observation utilizing a turbo-pumped sputter coater (Quorum Technologies, model Q150T). Cross-sectional SEM analyses (i.e. analyses of the interior of the foam) were carried out after samples freezing in liquid N_2 for 30-60 s and cutting with a scalpel blade parallel to the gas flow direction and perpendicular to the substrate top. The dimension of foam pores and ligaments, as well as the thickness of coating deposited on the foam struts were estimated by SEM images with the help of a dedicated software (Image J). Coating thickness values are the average of 8 samples (measurements on at least five cross-sectioned foam ligaments per sample).

The thickness of coatings deposited on borosilicate glass slides was measured using an Alpha-Step 500 KLA Tencor Surface profilometer . Measurements were repeated on three different samples produced in different experiments (five measurements on each sample).

Surface wettability was evaluated with a Ramé-Hart manual goniometer (model 100) by static water contact angle (WCA) measurements (5 µl drops). The reported WCA values are the average of measurements on three different samples produced in different experiments (five measurements for each sample).

Results and Discussion

Under the experimental conditions utilized in this work, the DBD operate in a filamentary regime. As shown in **Figure 2**, the DBD current signal, when no substrate is present, is composed of one main narrow peak and a secondary broad tailed peak per half cycle; even if all positive (and negative) peaks exhibit almost the same shape, amplitude, and position in the cycle, this current signal cannot be associated with a homogeneous regime since slight discharge filamentation phenomena were clearly detected by naked-eye.

Figure 1 and 2 report, respectively, the photographs and current signals of the DBD when 10 and 30 mm wide foam strips are located in the middle of the discharge region (i.e., direct plasma deposition), sandwiched between the dielectric-covered electrodes of the DBD system. As already described in the Experimental Section, it is worth mentioning that, using this configuration, during deposition the feed mixture is forced to flow through the interconnected porous structure of the foam, since the cross-sections of the foam strips perpendicularly to the gas flow direction and of the gas flow channel of the DBD system are identical (i.e., 120 mm × 5 mm). This allows obtaining the ignition of the discharge both outside the foam substrate and throughout its entire porous structure, as evident in Figure 1b and c.

The current signals of the DBD when the foam strips are located in the middle of the discharge region (Figure 2) slightly differ from that obtained without substrate under identical experimental conditions. The presence of the foam induces in fact a slight decrease of the main narrow peak and an increase of the broad tailed one, while the average power dissipated by the discharge remains unchanged (50 ± 2 W).

Figure 3 summarizes some general aspects of the surface chemical composition and morphology of the pristine 30 ppi PU foam used in this work. Results from XPS analysis show that the carbon, oxygen and nitrogen surface atomic concentrations are about 78%, 19% and 3%, respectively. The high resolution C1s XPS spectrum of the coating (Figure 3b) can be curve-fitted with the dominant hydrocarbon component (C−C/C−H) at 284.8 ± 0.2 eV, and other three peaks centered at 285.7 ± 0.2 eV (C-N), 286.5 ± 0.2 eV (C-O) and 289.0± 0.2 eV (very likely ascribed to both urethane and ester functionalities of the polyester polyol-based polyurethane material).

The photograph and the low magnification SEM image reported in Figure 3a and c, respectively, evidence the open-cell isotropic porous structure of the foam consisting of a three-dimensional continuous network of interconnected solid struts, also referred to as ligaments. The ligaments have the typical concave triangular cross-section (Figure 3d) of high porosity open-cell PU foams. The minimum ligament width varies in the range 140-220 μm, while the pores dimension ranges between 400 and 1300 μm.

A representative high resolution C1s XPS spectrum of the cross-section of a 10 mm wide foam strip, after a deposition time of 30 min, is shown in **Figure 4**a, while curve-fitting results are reported in **Table 1**. The C1s signal is curve-fitted with the typical components ascribed to the fluorinated groups of a plasma-deposited fluorocarbon coating[12,17-18] and, specifically, the peaks at 286.8 ± 0.2 eV (C-CF, including also possible contributions from C-O and C=O functionalities), 289.1 ± 0.2 eV (CF), 291.4 ± 0.2 eV (CF_2) and 293.5 ± 0.2 eV (CF_3); a weak hydrocarbon component (284.8 ± 0.2 eV) is also included (about 4% peak area) and could be due to both the underlying PU substrate and adventitious carbon. The possible substrate contribution to the C1s signal suggests that either the thickness of the deposited film is close to the sampling depth of XPS (4−10 nm) or that during sample preparation (i.e., sample cutting after plasma treatment) some untreated material was inevitably exposed and/or some damage of the coating occurred.

As reported in Table 1, in case of the foam cross-section, the peak area percentages ascribed to CF, CF_2 and CF_3 groups is greater than 20% and the XPS F/C ratio, calculated from curve-fitting results, is 1.39 ± 0.05. Interestingly, quite similar XPS results are obtained if the deposition is performed under identical processing conditions on a glass slide placed in the middle of the discharge region (Figure 4b and Table 1). Only minor differences can be detected and, specifically, a slightly higher F/C ratio (1.47 ± 0.3) and a lower contribution of the hydrocarbon component (peak area percentage below 2%) when a glass slide rather than the PU foam is used as substrate. Results from XPS analysis indicate also a very low oxygen surface atomic concentration (below 1%) for both plasma-treated substrates (i.e., PU foam and glass slide), reasonably ascribable to oxygen and water vapor contaminations in the Plexiglas chamber of the DBD reactor and/or to oxygen uptake upon post-deposition air exposure of the coating.

To assess the uniformity of the plasma treatment, XPS analyses were carried out at different positions on the plasma-treated 10 mm wide foam strips. In particular as illustrated in **Figure 5**a, besides the inner surfaces of the foam (i.e., cross-section), the outer surfaces directly exposed to the discharge ignited in the "free" gas gap (i.e., left and right), as well as the top and bottom sides in contact with the dielectric plates of the DBD cell were analyzed. For a deposition time of 30 min, good uniformity of the surface chemical composition was achieved over the entire foam substrate; in fact, as reported in **Table 2**, the XPS F/C ratio varies between 1.39 ± 0.05 and 1.45 ± 0.04, while the peak area percentage of the hydrocarbon component remains below 4%. Interestingly, thin film deposition occurs also on the top and bottom of the foam strips; this could be explained considering that, due to the complex 3D structure of the foam, substrate contact with the dielectric plates is only possible at some protruding points; therefore, the discharge (i.e., in the form of a surface discharge that spreads on the dielectric plate surface)[19] and/or depositing species can reach approximately the entire surface of the substrate.

Table 2 and Figure 5b report XPS results obtained for 10 mm wide foam strips with increasing the deposition time from 5 to 30 min. Overall, an increase of the fluorination degree of the plasma-treated foams can be observed as a function of the deposition time. For instance, as far as the interior of the foam is concerned (i.e., cross-section), with increasing the deposition time from 5 to 30 min the F/C ratio increases from 1.21 ± 0.10 to 1.39 ± 0.05 and the area percentage of the hydrocarbon component in the C1s spectra decreases from 9 ± 2% to 3.9 ± 0.7%. Considering the exterior of the foam and, for instance, the surfaces on the right side of the foam strips, the F/C ratio remains quite constant within the experimental error (1.37 ± 0.04 and 1.41 ± 0.04 at 5 and 30 min, respectively) and the percentage of the hydrocarbon component in the C1s spectra slightly decreases from 5.0 ± 1.2% to 2.8 ± 0.03%. For a deposition time of 5 min (i.e., the shorter deposition time used in this work), moderate changes in surface chemical composition moving from the outer to the inner surfaces of the plasma-treated foam can be observed, since the interior of the foam presents a lower fluorination degree (F/C ratios of 1.21 ± 0.10) than the exterior (F/C ratios from 1.27 ± 0.04 of 1.37 ± 0.04) .

To further investigate the chemical uniformity of the plasma treatment, larger substrates were used, and in particular foam strips having a width along the gas flow direction of 30 mm (**Figure 6**a). XPS analyses were carried out on the foam cross-section at different positions along the gas flow direction, and specifically at 5, 15 and 25 mm from the gas entrance into the foam (**Figure 6**a). XPS results summarized in **Table 3** and Figure 6b demonstrate that, for a deposition time of 30 min, the surface chemical composition of the foam cross-section does not change as a function of the position, i.e. as a function of the gas residence time into the substrate.

To gain insight into the influence that the ignition of the discharge within the porous structure of the foam can have in thin film deposition, a comparative experiment was performed locating a 10 mm wide foam strip downstream of the discharge region, close to the electrodes

edge. The high resolution C1s XPS signal reported in Figure 4c, corresponding to the cross-section of the foam treated for 30 min, shows that in this case the fluorination degree is considerably lower (F/C ratio = 1.03 ± 0.15) than in the direct approach (F/C ratio = 1.39 ± 0.05). In particular, the high resolution C1s spectrum of the downstream plasma-treated foam (Figure 4c and Table 1) shows reduced contributions from the fluorinated groups; the most abundant C1s signal component corresponds to the hydrocarbon peak ascribed to the underlying PU substrate (peak area percentage of 25%), pointing out that in this case a very thin fluorocarbon layer was likely deposited; moreover, the downstream plasma-treated foam presents a XPS atomic percentage of oxygen of about 4%, reasonably due in this case to the contribution of oxygen-containing moieties of the PU polymer. This evidence supports the hypothesis that the transport of thin film precursors (favored by the high total gas flow rate) can contribute to coating deposition within the foam interior; however, under direct deposition conditions, the ignition of the discharge within the porous structure of the substrate favors thin film growth into its interior at higher deposition rates.

Figure 7 reports representative SEM images of a 10 mm wide foam strip treated for 30 min in the middle of the discharge region. At low magnification, the plasma-treated (Figure 7a) and pristine (Figure 3c) foams seems identical and therefore it can be concluded that the overall porous architecture of the substrate was not modified by the plasma treatment.

SEM observation of cross-sectioned ligaments allowed obtaining full evidence of the presence of the coating within the interior of the plasma-treated foam. Figure 7c, d and e clearly show the fluorocarbon film deposited on the struts of the foam. Considering the roughly triangular cross-section of the ligaments (Figure 7b), the thickness of the coating seems to be greater on the vertices (Figure 7c) than on the sides (Figure 7d and e), in particular for a deposition time of 30 min average thickness values are 440 ± 80 nm and 170 ± 30 nm for ligament vertices and sides, respectively. No appreciable variation of the coating thickness was observed moving from the outer the inner surfaces of the foams as well as a function of the gas

residence time into the foam in case of 30 mm wide foam strips. The correlation of results from thickness measurements and XPS analyses for a deposition time of 30 min allows concluding that the PU substrate contribution to the XPS C1s signal is not due to a thickness of the deposited film close to the sampling depth of XPS and, instead, can be ascribed to the fact that during sample cutting after plasma treatment some untreated material is inevitably exposed and/or some damage of the coating occurs.

Under identical processing conditions, the thickness of the fluorocarbon coating deposited on glass slides placed in the middle of the DBD cell, in a region having a width of 50 mm and therefore greater than the maximum width of the foam strips used in this work, is 780 ± 30 nm.

Finally, the wettability of the pristine and plasma-treated substrates was evaluated (**Figure 8**). The picture in Figure 8a indicate that the pristine foam placed in a beaker containing water tends to absorb water and consequently remains below the water surface. On the contrary, the plasma-treated foam (30 min deposition time) freely floats on the surface of water and does not absorb water even if forcefully submerged. The plasma-treated foam shows hydrophobic behavior (Figure 8b) and is characterized by a static WCA of 133 ± 5°; the static WCA value of the fluorocarbon coating deposited on a flat glass substrate is 118 ± 5°.

Conclusion

In summary, a He/C_3F_6-fed atmospheric pressure DBD was used to deposit a fluorocarbon coating on a commercial PU foam characterized by porosity of about 97% and pore density of 30 ppi. During plasma processes, the discharge was ignited both outside the foam and throughout its entire 3D porous structure, to allow the deposition of a fluorocarbon coating on both the outer and inner surfaces of the substrate. XPS results showed moderate changes in

surface chemical composition moving from the exterior to the interior of the plasma-treated samples even after a relatively short treatment time (5 min). SEM observations revealed no changes to the overall porous architecture of the substrates and allowed estimating the thickness of the coating deposited on the struts of the foam.

While, at current stage of this research, we prefer not to make sweeping and hasty generalizations on the applicability of the proposed deposition process, we believe that the results obtained in this work uncover a new direction in surface processing of materials by atmospheric pressure cold plasmas. Future directions of this work include the investigation of different plasma conditions and feed mixtures, the use of foams characterized by higher pore density and, therefore, reduced pore dimension, the optimization of the final properties of the plasma-treated foams for application as special wettable materials, selective adsorbents and heterogeneous catalysts.

Acknowledgements: The research is supported by the Italian Ministry for Education, University and Research (MIUR), under grants PRIN 2009, PON01_02239 and PONa3_00369, PON02_00576_3333604, and Regione Puglia under grant no. 51 “LIPP” within the Framework Programme Agreement APQ “Ricerca Scientifica”, II atto integrativo - Reti di Laboratori Pubblici di Ricerca. The Danilo Benedetti, Savino Cosmai and Teresa Lasalandra are gratefully acknowledged for the skilful technical assistance.

Received: ; Revised: ; Published online: ; DOI:

Keywords: dielectric barrier discharges (DBD); fluoropolymers; plasma-enhanced chemical vapor deposition (PECVD); polyurethane foam

[1] a) J. J. A. Barry, M. M. C. G. Silva, K. M. Shakesheff, S. M. Howdle, M. R. Alexander, *Adv. Funct. Mater.* **2005**, *15*, 1134; b) J. J. A. Barry, D. Howard, K. M. Shakesheff, S. M. Howdle, M. R. Alexander, *Adv. Mater.* **2006**, *18*, 1406.

[2] H. Zhang, W. J. Suszynski, K. V. Agrawal, M. Tsapatsis, S. Al Hashimi, L. F. Francis, *Ind. Eng. Chem. Res.* **2012**, *51*, 9250.

[3] a) Q. Zhu, Q. Pan, F. Liu, *J. Phys. Chem. C* **2011**, *115*, 17464; b) P. Calcagnile, D. Fragouli, I. S. Bayer, G. C. Anyfantis, L. Martiradonna, P. D. Cozzoli, R. Cingolani, A. Athanassiou, *ACS Nano* **2012**, *6*, 5413.

[4] W. Li, P. Bollini, S. A. Didas, S. Choi, J. H. Drese, C. W. Jones, *ACS Appl. Mater. Interfaces* **2010**, *2*, 3363.

[5] P. Guo, S. Zhai, Z. Xiao, Q. An, *J. of Coll. Interface Sci.* **2015**, *446*, 155.

[6] M. V. Twigg, J. T. Richardson, *Ind. Eng. Chem. Res.* **2007**, *46*, 4166.

[7] R. Davis, Y.-C. Li, M. Gervasio, J. Luu, Y. S. Kim, *ACS Appl. Mater. Interfaces* **2015**, *7*, 6082.

[8] G. L. Vignoles, C. Gaborieau, S. Delettrez, G. Chollon, F. Langlais, *Surf. Coat. Technol.* **2008**, *203*, 510.

[9] Y. Wang, G. A. Sotzing, R. A. Weiss, *Chem. Mater.* **2008**, *20*, 2574.

[10] U. Zavyalova, F. Girgsdies, O. Korup, R. Horn, R. Schlögl, *J. Phys. Chem. C* **2009**, *113,* 17493.

[11] a) F. Intranuovo, E. Sardella, R. Gristina, M. Nardulli, L. White, D. Howard, K. M. Shakesheff, M. R. Alexander, P. Favia, *Surf. Coat. Technol.* **2011**, *205*, S548; b) F. Intranuovo, R. Gristina, F. Brun, S. Mohammadi, G. Ceccone, E. Sardella, F. Rossi, G. Tromba, P. Favia, *Plasma Process. Polym.* **2014**, *11*, 184.

[12] a) E. R. Fisher, *ACS Appl. Mater. Interfaces* **2013**, *5*, 9312; b) M. J. Hawker, A. Pegalajar-Jurado, E. R. Fisher, *Langmuir* **2014**, *30*, 12328.

[13] M. Zelzer, D.d Scurr, B. Abdullah, A. J. Urquhart, N. Gadegaard, J. W. Bradley, M. R. Alexander, *J. Phys. Chem. B* **2009**, *113,* 8487.

[14] M. A. Lieberman, A. J. Lichtenberg, *Principles of Plasma Discharges and Materials Processing*, Wiley, Hoboken, NJ, USA **2005**.

[15] a) M. Kraus, B, Eliasson, U. Kogelschatz, A. Wokaun, *Phys. Chem. Chem. Phys.* **2001**, *3*, 294; b) K. Hensel, V. Martisovits, Z. Machala, M. Janda, M. Lestinsky, P. Tardiveau, A. Mizuno, *Plasma Process. Polym.* **2007**, *4*, 682; c) K. Hensel, *Eur. Phys. J. D* **2009**, *54*, 141.

[16] a) R. Pothiraja, N. Bibinov, P. Awakowicz, *J. Phys. D: Appl. Phys.* **2011**, *44*, 355206; b) M. Eichler, K. Nagel, P. Hennecke, C.-P. Klages, *Plasma Process. Polym.* **2012**, *9*, 1160; c) M. Bashir, S. Bashir, J. M. Rees, W.. B. Zimmerman, *Plasma Process. Polym.* **201**4, 11, 279.

[17] a) F. Fanelli, R. d'Agostino, F. Fracassi*, Plasma Process. Polym.* **2007**, *4*, 797; b) F. Fanelli, G. Di Renzo, F. Fracassi, R. d'Agostino, *Plasma Process. Polym.* **2009**, *6*, S503; c) F. Fanelli, R. d'Agostino, F. Fracassi, *Plasma Process. Polym.* **2011**, *8*, 557.

[18] a) B. Nisol, F.Reniers, *J. Electron Spectrosc. Relat. Phenom.*, DOI: 10.1016/j.elspec.2015.05.002; b) J. Hubert, N. Vandencasteele, J. Mertens, P. Viville, T. Dufour, C. Barroo, T. Visart de Bocarme, R. Lazzaroni, F. Reniers, *Plasma Process. Polym.*, DOI: 10.1002/ppap.201500025.

[19] U. Kogelschatz*, Plasma Chem. Plasma Process.* **2003**, *23*, 1.

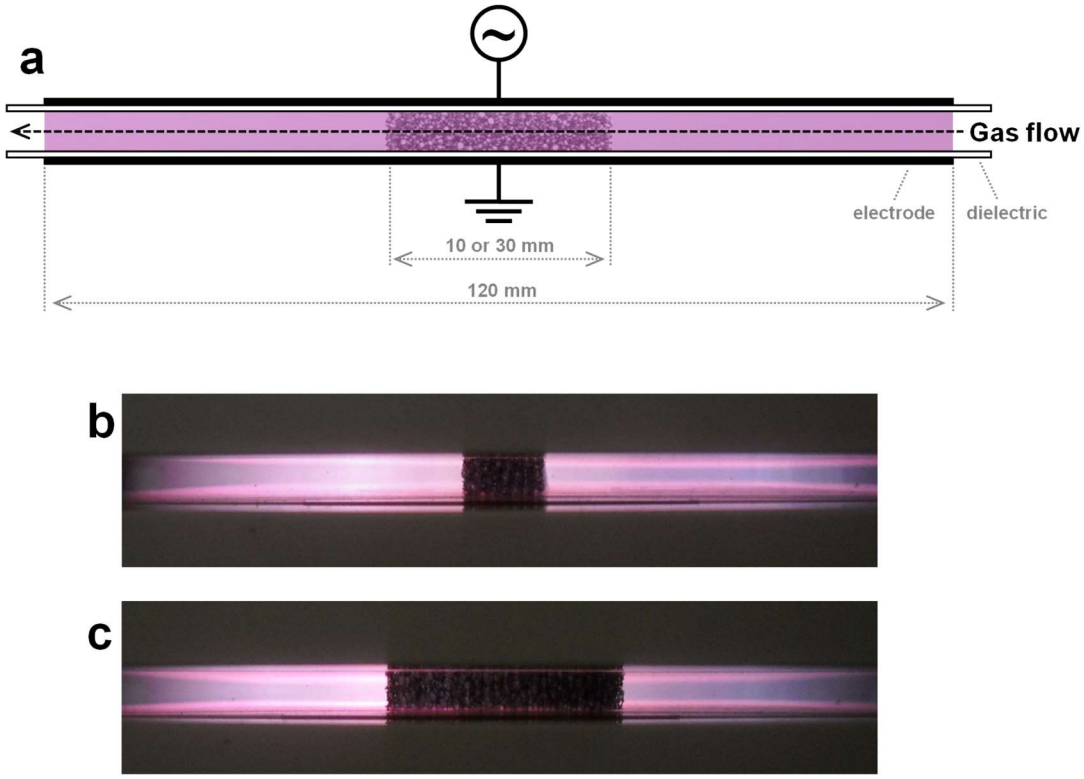

Figure 1. (a) Schematic diagram showing the side view of the parallel plate DBD cell used for thin film deposition on PU foams; photographs of the DBD taken when foam strips having a width of 10 mm (b) and 30 mm (c) along the gas flow direction are positioned in the middle of the discharge region.

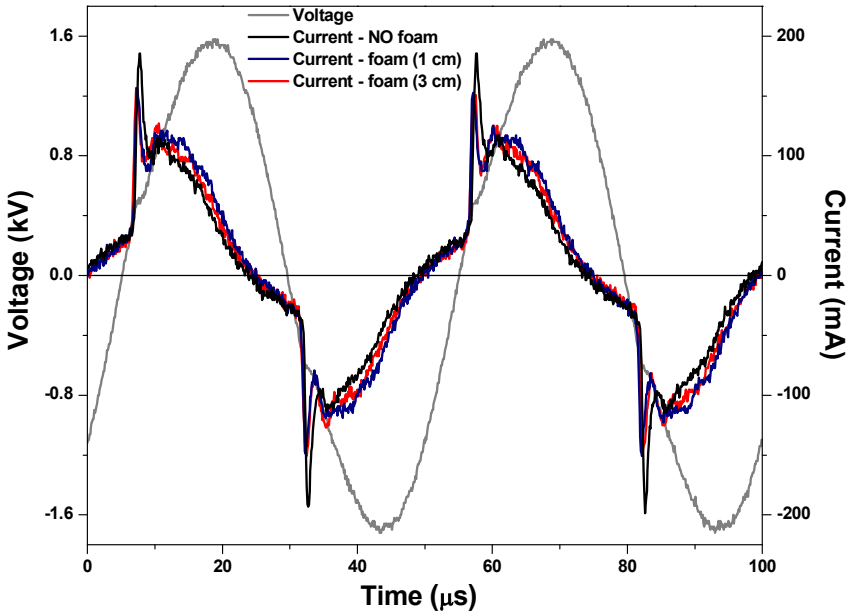

Figure 2. Voltage and current signals of the DBD when no substrate is present and when foam strips having a width of 10 and 30 mm along the gas flow direction are positioned in the middle of the discharge region.

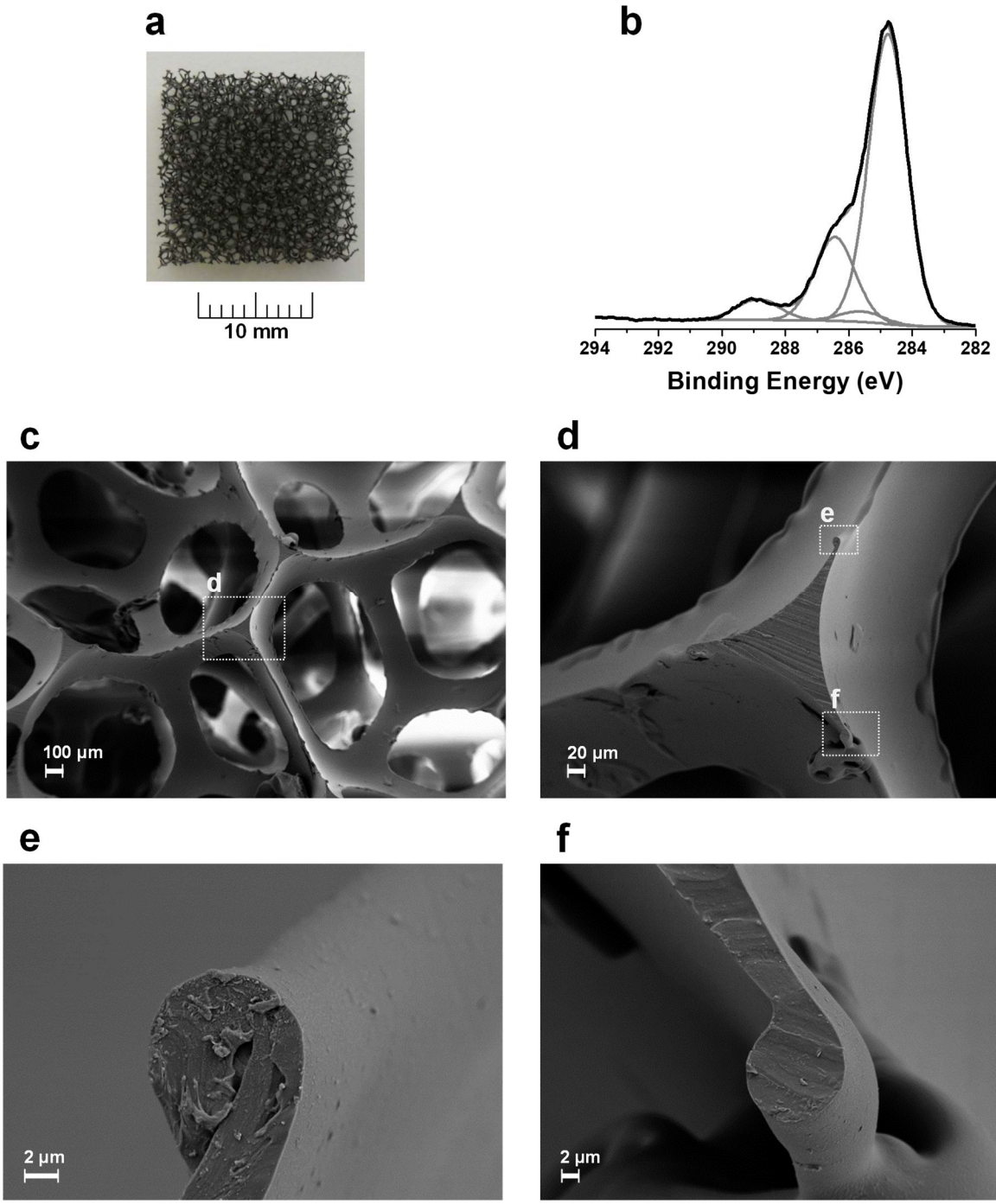

Figure 3. Photograph (a), high resolution C1s XPS signal (b) and representative SEM images at different magnification (c-f) of the pristine PU foam.

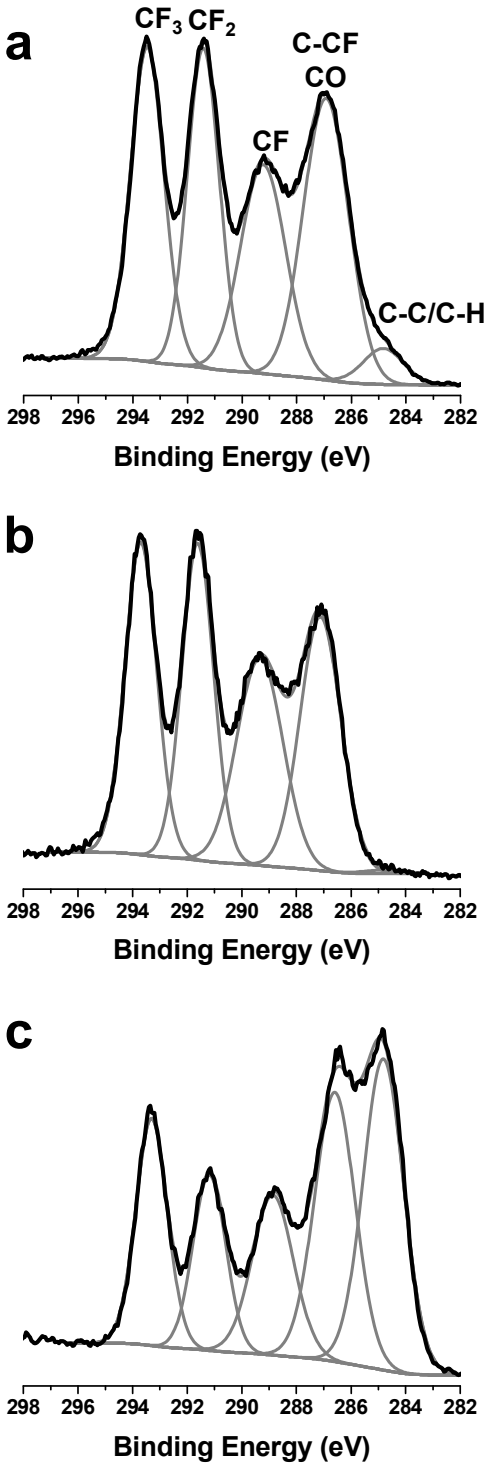

Figure 4. High resolution C1s XPS signals: (a) cross-section of the plasma-treated PU foam positioned during deposition in the middle of the discharge region (direct plasma deposition); (b) fluorocarbon film deposited on a glass slide positioned during deposition in the middle of the discharge region (direct plasma deposition), (c) cross-section of the plasma-treated PU foam positioned downstream of the discharge region. Width of the foam strips = 10 mm; deposition time = 30 min.

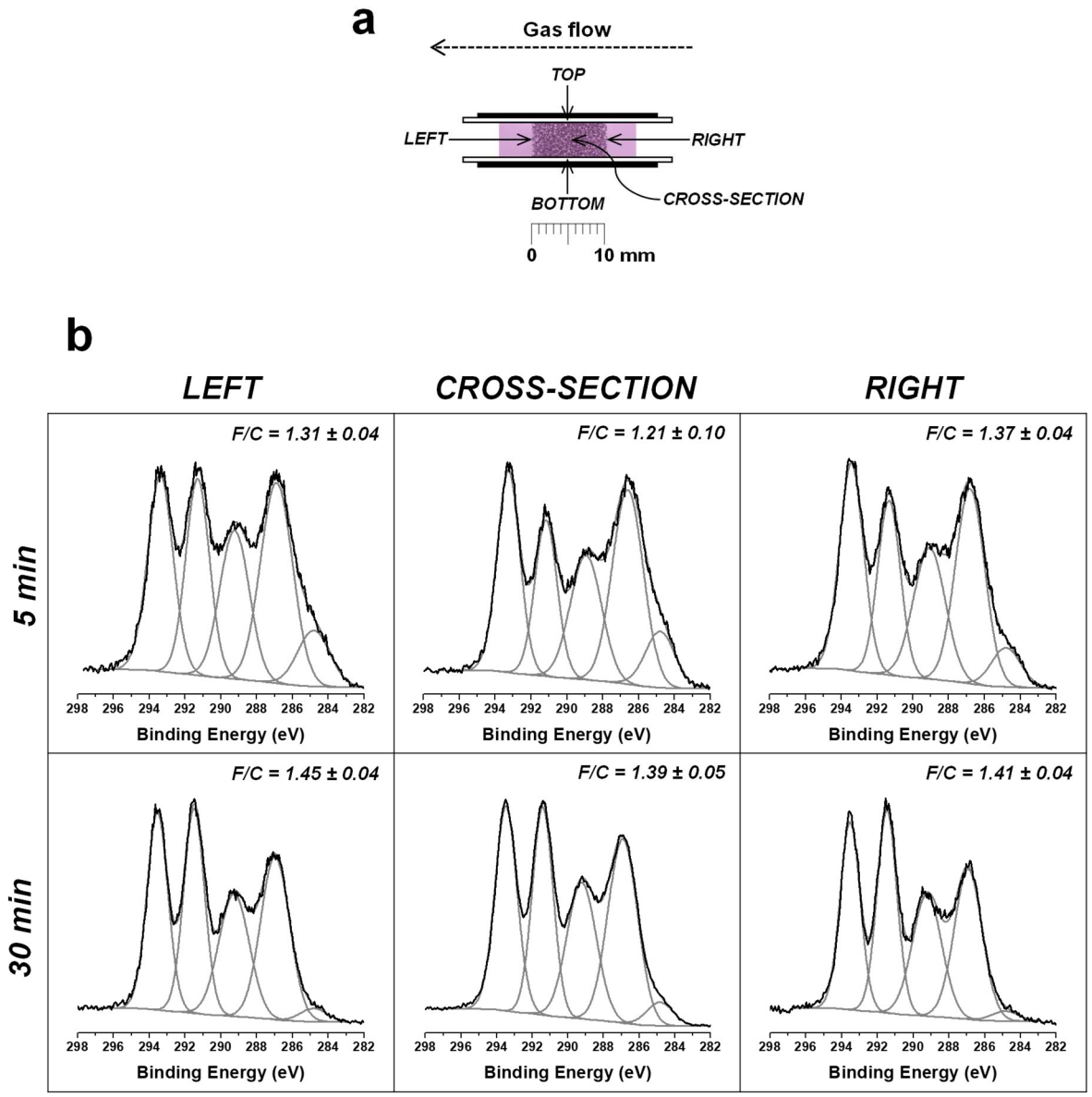

Figure 5. (a) Schematic representation showing the different positions analyzed by XPS on 10 mm wide foam strips; (b) high resolution C1s XPS signals of the outer (left and right side) and inner (cross-section) surfaces of the plasma-treated foam at deposition times of 5 and 30 min.

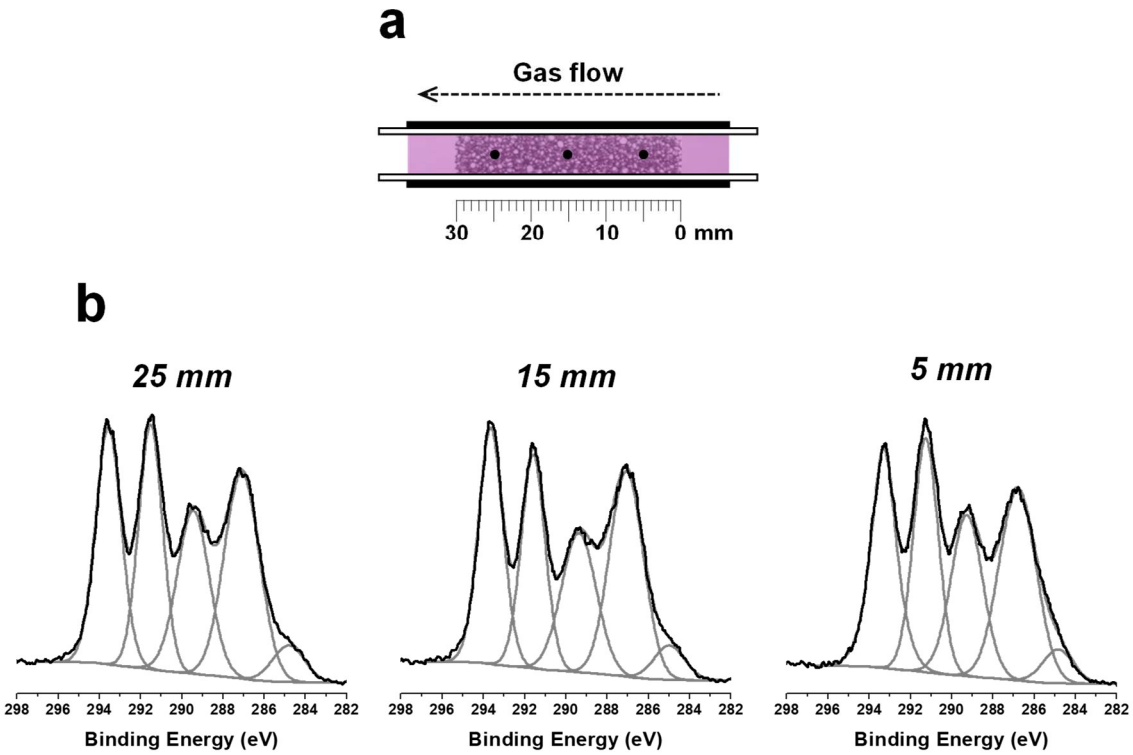

Figure 6. (a) Schematic illustration showing the different positions analyzed by XPS on the cross-section of a 30 mm wide foam strip; (b) high resolution C1s XPS spectra of the foam cross-section at different positions (i.e., 5, 15 and 25 mm) along the gas flow direction (the 0 mm position corresponds to gas entrance into the porous substrate).

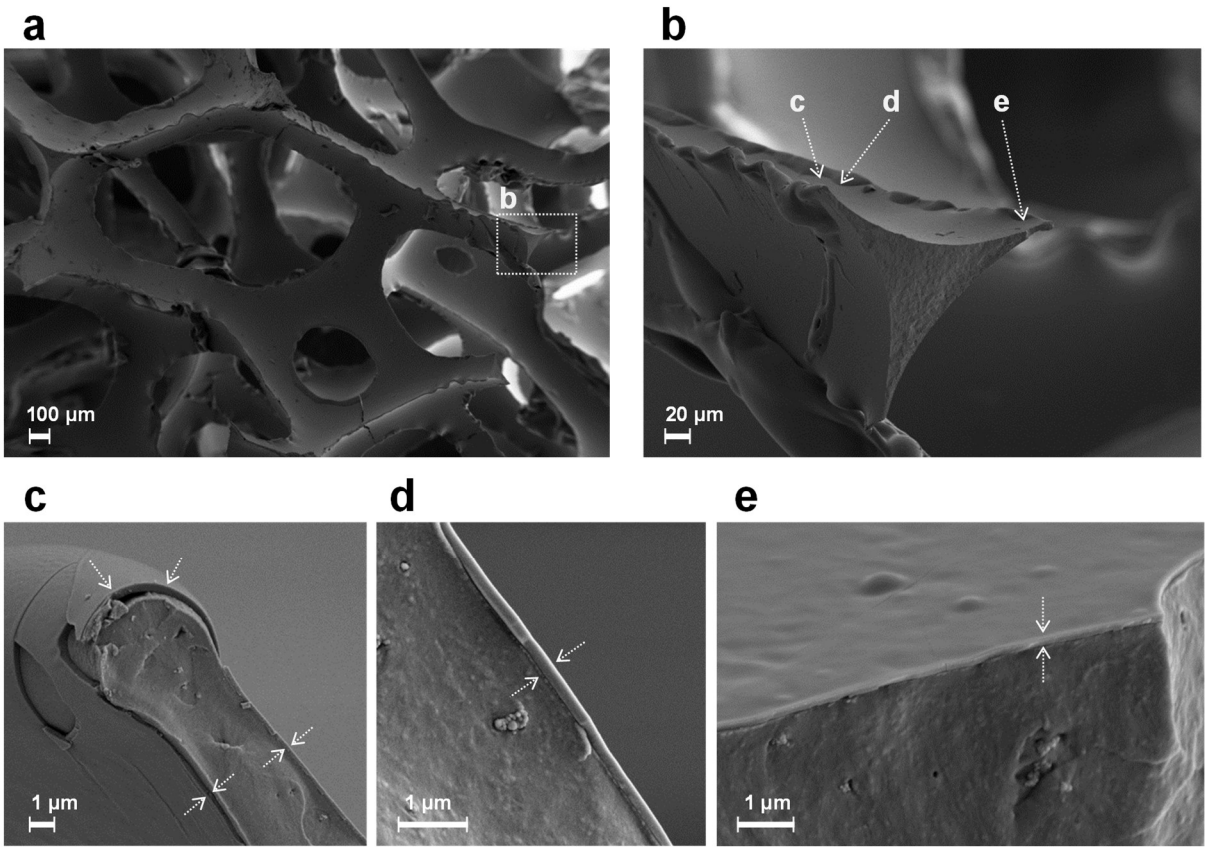

Figure 7. SEM images corresponding to the cross-section of a 10 mm wide foam strip treated for 30 min in the middle of the discharge region: (a) low magnification image; (b) cross-sectioned ligament; (c-e) different regions of the cross-sectioned ligament where the deposited coating is clearly visible (indicated by white arrows).

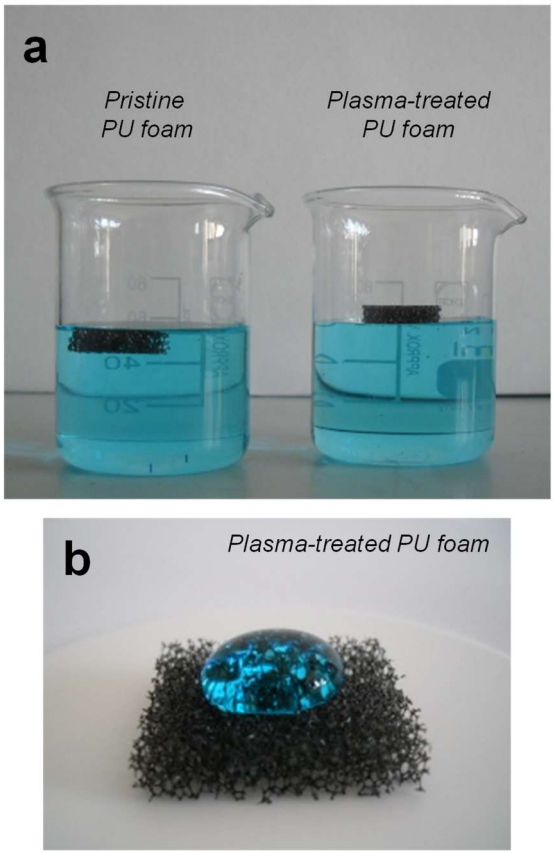

Figure 8. (a) Photograph of the pristine and plasma-treated foams placed in a glass beaker filled with water. (b) Photograph of a 0.5 mL water drop deposited on a plasma-treated foam. Water was dyed with methylene blue for better visualization.

Table 1. Curve-fitting results of the C1s XPS spectra corresponding to (a) the cross-section of the plasma-treated PU foam positioned in the middle of the discharge region during deposition (direct plasma deposition); (b) the fluorocarbon film deposited on a glass slide positioned in the middle of the discharge region (direct plasma deposition), (c) the cross-section of the plasma-treated PU foam positioned downstream of the discharge region (downstream plasma deposition). Width of the foam strips = 10 mm; deposition time = 30 min.

	Substrate/plasma deposition	**C-C/C-H [%]**	**C-CF/CO [%]**	**CF [%]**	**CF_2 [%]**	**CF_3 [%]**	**F/C**
a	PU foam/direct	3.9 ± 0.7	28.0 ± 1.4	21.2 ± 0.5	22.6 ± 0.8	24.3 ± 1.3	1.39 ± 0.05
b	Glass/direct	0.7 ± 0.2	26.5 ± 0.5	23.6 ± 0.2	24.2 ± 0.5	25.0 ± 0.3	1.47 ± 0.03
c	PU foam/downstream	25 ± 5	25 ± 2	16 ± 2	15 ± 2	19 ± 2	1.03 ± 0.15

Table 2. Curve-fitting results of the high resolution XPS C1s spectra of 10 mm wide plama-treated foam strips as a function of the deposition time (5, 10 and 30 min). Spectra are taken at different position on the foam substrate as illustrated in Figure 5a.

Deposition time [min]	**Position**	**C-C/C-H [%]**	**C-CF/CO [%]**	**CF [%]**	**CF_2 [%]**	**CF_3 [%]**	**F/C**
5	Cross-section	9 ± 2	32 ± 2	19.0 ± 1.5	18.0 ± 1.0	22 ± 2	1.21 ± 0.10
	Right	5.0 ± 1.2	29 ± 2	20.0 ± 1.0	21.5 ± 2	24.5 ± 1.0	1.37 ± 0.04
	Left	7 ± 2	29 ± 3	20.0 ± 0.5	21 ± 2	23.0 ± 0.5	1.31 ± 0.04
	Top	9.0 ± 1.0	28.5 ± 1.0	20.5 ± 0.8	20.0 ± 1.5	22.0 ± 0.5	1.27 ± 0.04
	Bottom	7.5 ± 1.0	29.0 ± 1.0	19.5 ± 1.2	21.0 ± 1.0	23.0 ± 1.5	1.31 ± 0.05
10	Cross-section	7 ± 3	29.5 ± 0.8	19.5 ± 1.1	20.0 ± 1.0	24 ± 2	1.32 ± 0.03
	Right	2.5 ± 0.5	28.9 ± 1.0	21.4 ± 0.5	22.9 ± 0.5	24.3 ± 0.5	1.40 ± 0.03
	Left	2.7 ± 0.5	29 ± 2	20.6 ± 0.6	22.3 ± 1.0	25.4 ± 0.5	1.41 ± 0.04
	Top	5.0 ± 1.0	31 ± 2	20.2 ± 0.6	21.2 ± 1.2	22.6 ± 0.5	1.30 ± 0.04
	Bottom	6 ± 2	31.0 ± 1.0	19.0 ± 0.5	20.0 ± 1.5	24.0 ± 1.5	1.31 ± 0.05
30	Cross-section	3.9 ± 0.7	28.0 ± 1.4	21.2 ± 0.5	22.6 ± 0.8	24.3 ± 1.3	1.39 ± 0.05
	Right	2.8 ± 1.1	27.7 ± 0.4	21.3 ± 0.9	24.7 ± 0.4	23.5 ± 1.5	1.41 ± 0.04
	Left	2.0 ± 0.5	26.4 ± 0.5	22.5 ± 0.5	25.3 ± 0.5	23.8 ± 1.5	1.45 ± 0.04
	Top	3.1 ± 0.6	25.6 ± 0.8	22.2 ± 2	24.9 ± 0.8	24.2 ± 1.2	1.45 ± 0.04
	Bottom	3.2 ± 0.5	29.0± 21.3	21.3 ± 0.9	21.4 ± 2	25.1 ± 1.5	1.39 ± 0.05

Table 3. Curve-fitting results of the high resolution C1s XPS spectra corresponding to different positions on the cross-section of a 30 mm wide foam strip; analyses are carried out along the gas flow direction at 5, 15 and 25 mm from the gas entrance into the foam substrate as illustrated in Figure 6a.

Position [mm]	**C-C/C-H [%]**	**C-CF/CO [%]**	**CF [%]**	**CF_2 [%]**	**CF_3 [%]**	**F/C**
5	4.0 ± 1.0	28 ± 2	21.0 ± 1.5	23.5 ± 1.5	23.5 ± 1.5	1.39 ± 0.03
15	4.5 ± 1.5	29 ± 2	20.5 ± 0.7	21.5 ± 2	24.5 ± 1.0	1.37 ± 0.04
25	4.5 ± 1.0	28 ± 2	20.5 ± 1.2	23 ± 2	24 ± 2	1.39 ± 0.03

Fluorocarbon coatings are deposited on open-cell polyurethane foams using an atmospheric pressure dielectric barrier discharge fed with helium and hexafluoropropene. The discharge is ignited both outside and inside the three-dimensional porous structure of the foam, so that thin film deposition can be achieved on both its outer and inner surfaces.

F. Fanelli, * F. Fracassi

Thin film deposition on open-cell foams by atmospheric pressure dielectric barrier discharges